Desalination and Water Treatment
www.deswater.com
doi: 10.1080/19443994.2015.1021844

57 (2016) 8372–8388
April

Taylor & Francis
Taylor & Francis Group

Cationic and anionic dye removal from aqueous solution using montmorillonite clay: evaluation of adsorption parameters and mechanism

Ponchami Sharma[a], Dipankar J. Borah[a], Pankaj Das[b], Manash R. Das[a,*]

[a]*Materials Science Division, CSIR-North East Institute of Science and Technology, Jorhat 785006, Assam, India, Tel. +91 9864550510; email: ponchi.du@gmail.com (P. Sharma), Tel. +91 9706408960; email: dipankarjyotibora@gmail.com (D.J. Borah), Tel. +91 9957178399; Fax: +91 376 2370011; emails: mrdas@rrljorhat.res.in, mnshrdas@yahoo.com (M.R. Das)*

[b]*Department of Chemistry, Dibrugarh University, Dibrugarh 786004, Assam, India, Tel. +91 9435394373; email: pankajd29@yahoo.com*

Received 22 May 2014; Accepted 12 February 2015

ABSTRACT

This paper deals with the removal of methyl green, a cationic dye, and methyl blue, an anionic dye, from aqueous system by adsorption onto the montmorillonite clay. The effect of different experimental conditions such as time, adsorbate concentrations, pH, temperature, and presence of other ions has been investigated. In order to understand the adsorption behavior of the dye molecules onto montmorillonite, the kinetics of the adsorption data were analyzed using different models such as pseudo-first-order, pseudo-second-order, intraparticle diffusion, Boyd, Elovich, Richi, and Bajpai model. This study shows that the adsorption maximum reached at 60 min and follows the pseudo-second-order kinetics. The adsorption isotherm has been investigated in the pH range of 4–9 at 25°C and analyzed with different models namely Langmuir, Freundlich, Sips, Toth, Temkin, Scatchard, and Dubinin and Raduskevich (D–R) models. The thermodynamic parameters such as the Gibbs free energy (ΔG°), enthalpy (ΔH°), and entropy (ΔS°) changes were calculated. The interaction of dye molecules onto montmorillonite has been investigated by X-ray diffraction analysis which indicates that adsorption takes place mainly into the interlayer region of the clay. Maximum removal of methyl green and methyl blue dye molecules up to 68.35 and 95.95%, respectively was achieved by adsorption of the dye molecules onto montmorillonite clay at pH 5 and 35°C.

Keywords: Montmorillonite clay; Adsorption; Kinetics; Isotherm; Thermodynamics

1. Introduction

Dyes are considered as one of the widely used materials in modern world. A number of industries such as textile, paper, food, leather, plastic, cosmetic, printing etc. extensively use dyes. The release of colored wastewater from these industries may present an ecotoxic hazard and have potential danger of bioaccumulation [1]. Therefore, the dye containing wastewater must pass through some cleaning treatment before releasing into main water stream. Over the years, a number of technologies such as trickling filter, active sludge, chemical coagulation, adsorption, photodegradation, nanofiltration etc. have been widely

*Corresponding author.

studied for dye removal from aqueous system [2]. Adsorption based processes have a special place in this regard due to their simplicity and cost effectiveness. Recent studies on adsorption technology have focused on the development of low cost and easily available adsorbent materials [3]. Use of clay minerals as alternative adsorbents in wastewater treatments has several advantages such as low cost, wide availability, non-toxicity, and high potential of ion exchange for charged pollutants etc. [3–8]. Adsorption of dye molecules onto clay minerals such as montmorillonite, bentonite, perlite etc. have been reported by a number of researchers [3,4,7,8]. Das et al. group has focused on the evaluation of different adsorption parameters for adsorption of anionic and cationic dye molecules onto different adsorbent in order to find out some efficient adsorbent materials for removal of these dye molecules from aqueous system. Recently, these authors have investigated the adsorption of dye molecules onto graphene oxide (GO) and reduced graphene oxide (rGO) nanosheets [9,10]. GO and graphene have attracted the researchers as new adsorbent materials for removal of dye molecules from aqueous system due to their large surface area, layered structure, and possibility for electrostatic charge–charge interaction [9–14].

In order to develop an adsorbent material with optimum efficiency, detailed investigations of adsorption parameters, effect of different factors on adsorption, understanding the adsorption mechanism and comparison of adsorption efficiency with other adsorbent materials are very important. Montmorillonite and other clay minerals are well known as adsorbent materials due to their high surface area, chemical, and mechanical stability, ion-exchange capacity and layered structure. As already discussed, GO and rGO also posses high surface area and layered structure. Due to such structural similarities of GO, rGO, and montmorillonite clay, adsorption of a cationic dye molecule, methyl green, and an anionic dye molecule, methyl blue onto the montmorillonite clay have been studied and results are compared with adsorption of these two dye molecules onto GO and rGO nanosheets. Methyl green (CI 42585) and methyl blue (CI 42755) fall under the class of triarylmethane. Triarylmethane dyes are reported to be toxic and carcinogenic and therefore must be eliminated from wastewater before surface discharging [15]. The adsorption mechanism is evaluated with kinetics, isotherm, effect of pH, temperature, presence of different electrolytes, FTIR, and XRD analysis.

2. Experimental

2.1. Materials

Montmorillonite clay (Sigma–Aldrich, India), hydrochloric acid (AR grade, Qualigens, India), NaOH (99%, Qualigens, India), ascorbic acid (99%, Fisher Scientific, India), methyl green (Loba Chemie, India), and methyl blue (Loba Chemie, India) were used as received. Deionized water was used throughout the whole experiment.

2.2. Characterization of montmorillonite clay

The montmorillonite clay was characterized by FTIR, XRD, SEM-EDX, and DTA-TGA analysis. The FTIR spectra were recorded with an IR Affinity-1, Shimadzu, Japan FTIR spectrophotometer in KBr pellate. In all cases, the spectra were recorded with 200 scanning and 4 cm^{-1} spectral resolutions. X-ray diffraction (XRD) measurement was carried out by Rigaku X-ray diffractometer (Model: ULTIMA IV, Rigaku, Japan) with CuKα X-ray source (λ = 1.54056 Å) at a generator voltage 40 kV, a generator current 40 mA with the scanning rate 2 min^{-1}. Thermogravimetric analysis (TGA) of montmorillonite clay was carried out in a TA-SDT (Model: Q600DT, TA Instruments, USA) Thermogravimetric analyzer at a rate of 5°C rise in temperature per minute. The SEM-EDX analysis was carried out in a JEOL JSM (Singapore) microscope of model 6,390 LV.

2.3. Preparation of dye solution

The methyl green and methyl blue dye of concentration 5 mM were taken as stock solution for the experiments. The pH of the stock dye solutions were fixed at the required value using a pH meter (μ-pH system 362, Systronics, India) calibrated with standard buffer solutions of pH 4, 7, and 9. Dye solutions of different initial concentrations were prepared for the experiments by diluting the stock solution in accurate amount.

2.4. Adsorption kinetics

The effect of time on adsorption of the dye molecules were studied by carrying out the adsorption kinetic experiments at pH 5 and at four different temperatures (18, 25, 30, and 35°C) in aqueous medium (initial dye concentration: 0.2 mM). The kinetic experiments were performed by adopting same procedure reported elsewhere [9,10]. The adsorption capacity at the time t, q_t was determined using the Eq. (1)

$$q_t = (C_0 - C_e)V/m \quad (1)$$

where C_0 is the initial concentration of the dye molecules, C_0 is the concentration of the dye molecules at time t, V is the total volume of the solution, and m is the mass of the montmorillonite clay used as adsorbent.

2.5. Adsorption isotherm

The batch adsorption isotherm experiments were carried out in the pH range 4–9 and at 25°C. The experimental procedure adopted for isotherm study is akin to that of our previous work [9,10].

3. Results and discussion

3.1. Characterization of montmorillonite clay

Preliminary characterization of the Montmorillonite clay was carried out using FTIR, SEM–EDX, and XRD analysis. The FTIR spectrum of the clay is presented in Fig. 1. The bands at 3,447 and 1,602 cm^{-1} are due to –OH stretching of water [4,16]. The bands at 1,057 and 792 cm^{-1} are due to Si–O stretching. Al–O–Si deformation and Si–O–Si deformation shows bands at 527 and 467 cm^{-1} respectively [16].

Presence of Si, Al and O in the montmorillonite clay was further confirmed by SEM-EDX pattern (Fig. 2) The XRD pattern indicates the presence of Illite–montmorillonite-type structure (JCPDS 00-35-0652). The XRD pattern of the clay is shown in Fig. 3.

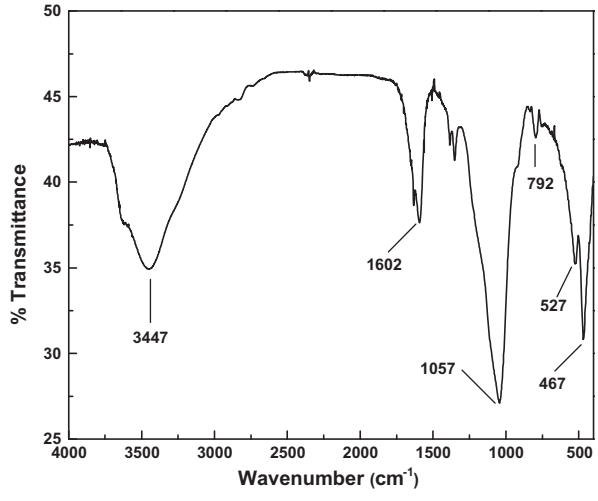

Fig. 1. FTIR spectrum of montmorillonite clay.

The TGA curve of montmorillonite clay shows a weight loss at 150°C due to evaporation of water (Fig. 4) [4,16]. Another weight loss at 670°C occurs due to loss of structural hydroxyl groups [4,16].

The surface area and average pore size of the montmorillonite clay was found to be 249 m^2/g and 38.34 nm, respectively as determined from the BET isotherm curve (Fig. 5).

3.2. Adsorption kinetics

The influence of time on adsorption of the dye molecules onto the montmorillonite clay in aqueous medium has been studied at pH 5 and at four different temperatures (18, 25, 30, and 35°C). The removal efficiency of methyl green and methyl blue dye molecules was found to be 50.75% and 67.60%, respectively at 18°C which increases up to 68.35% and 95.95%, respectively at 35°C. Fig. 6 represents the plot of adsorption capacity (q_t) vs. time which shows that the kinetic equilibrium for adsorption of the dye molecules onto the clay is reached at 60 min and the adsorption capacity increases with the increase in temperature. The adsorption capacity gradually decreases after attaining equilibrium at all four temperatures which may be attributed to the fact that desorption of the dye molecules takes place from the adsorbent surface. Occurrence of such desorption phenomenon after equilibrium indicates physical nature of adsorption process for which the dye molecule tends to go back to the solution after attaining equilibrium. Such desorption was also observed for adsorption of these two dye molecules onto GO and rGO nanosheets [9,10]. The kinetic data were analyzed with six different models namely pseudo-first-order, pseudo-second-order (linear), pseudo-second-order (non-linear), Elovich, Richi, and Bajpai kinetic models [17–22]. The plots for these kinetic models are shown in Figs. 7(a)–(e) and 8(a)–(e). The adsorption kinetic parameters were calculated from the models and presented in Table 1. The summery of these kinetic models are presented in Table 2. The R^2 values of the pseudo-second-order model (linear) more closely approaches to unity than the other kinetic models. It is also observed that the experimental q_e values and the calculated q_e values are more closer in pseudo-second-order model (linear) compared to other models. Therefore, it is concluded that pseudo-second-order model (linear) is the best fit model among all the kinetic models. Similar results were obtained for the adsorption of methyl green and methyl blue dye molecules onto the GO and rGO nanosheets [9,10].

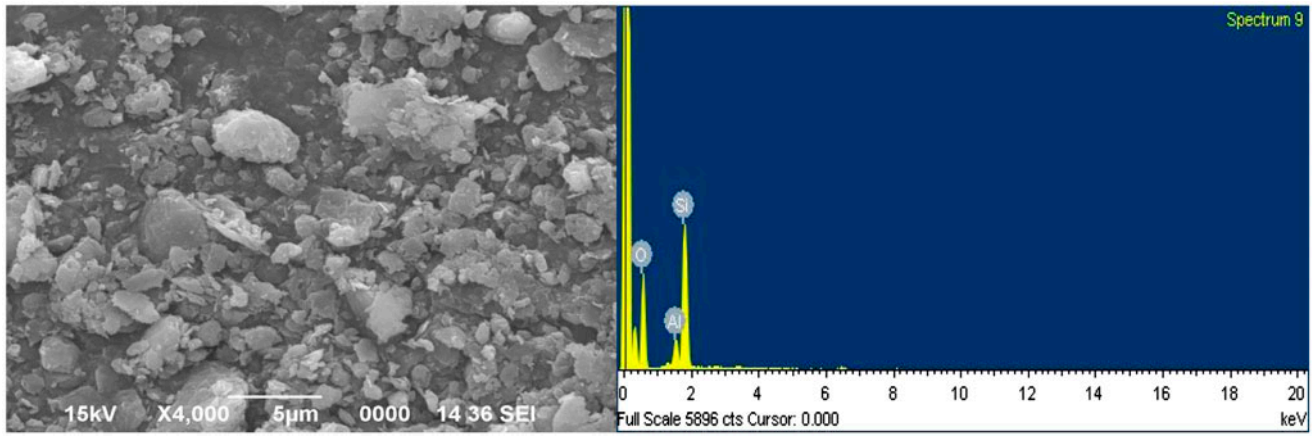

Fig. 2. SEM–EDX pattern of montmorillonite clay.

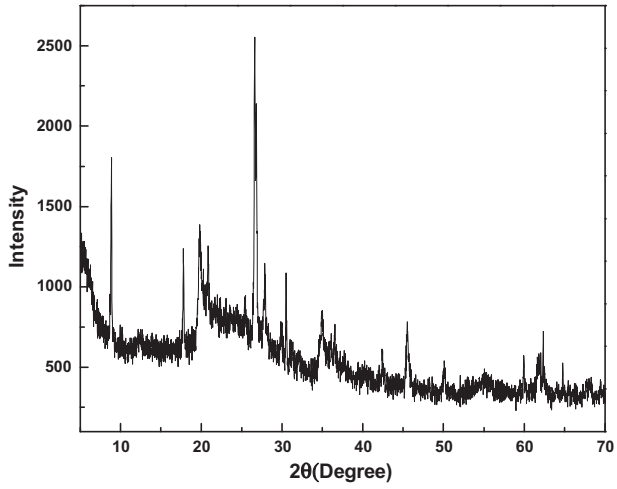

Fig. 3. XRD pattern of montmorillonite clay.

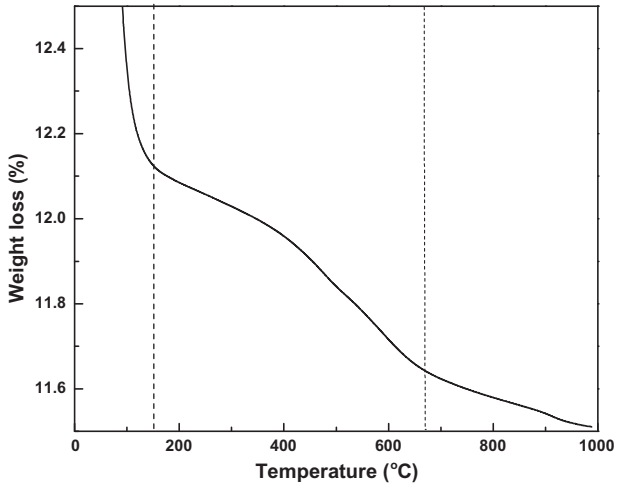

Fig. 4. TGA pattern of montmorillonite clay.

3.3. Thermodynamic study

The thermodynamics of the adsorption of methyl green and methyl blue dye molecules onto the montmorillonite clay was studied by performing the adsorption experiments in the temperature range (18–35)°C at pH 5. The variation of adsorption capacity of methyl green and methyl blue dye molecules with temperature is shown in Fig. 9. In common practice the thermodynamic parameters, namely standard Gibbs free energy change (ΔG°), enthalpy change (ΔH°), and entropy change (ΔS°) of an adsorption process are calculated by using the equations [23].

$$K_d = q_e/C_e \tag{2}$$

$$\Delta G^\circ = -RT\ln K_d \tag{3}$$

$$\ln K_d = \Delta S^\circ/R - \Delta H^\circ/RT \tag{4}$$

where K_d is the distribution coefficient (L/g), T is the temperature (K), and R is the gas constant (8.314 J/K mol), respectively. ΔH° and ΔS° are calculated from the slope and intercept of the plot of ln K_d vs. T^{-1}. However, use of K_d with dimension in calculation of thermodynamic parameters contains some errors [24,25]. Such errors can be avoided by multiplying K_d by 1,000 if the adsorption takes place from aqueous solution, whereby K_d becomes dimensionless (since, density of water ~1 or 1,000 g/L) [25]. Therefore, Eqs. (3) and (4) can be modified as

$$\Delta G^\circ = -RT\ln\,(1,000\,K_d) \tag{5}$$

$$\ln(1,000\,K_d) = \Delta S^\circ/R - \Delta H^\circ/RT \tag{6}$$

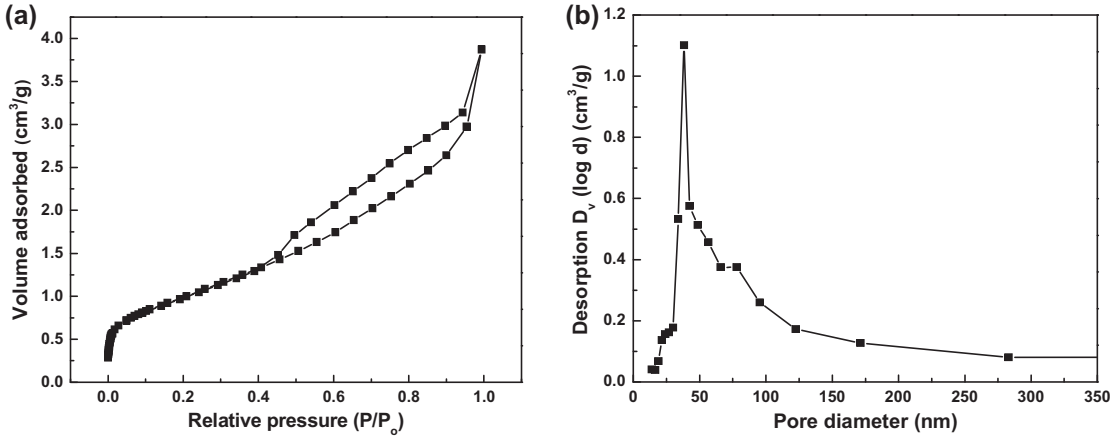

Fig. 5. (a) N_2 adsorption–desorption isotherm and (b) Pore volume plot of montmorillonite clay.

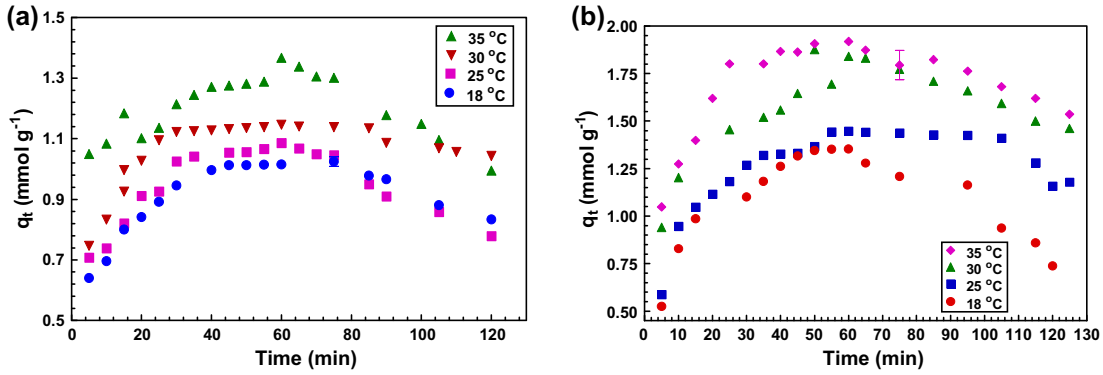

Fig. 6. Plot of adsorption capacity vs time for adsorption of (a) methyl green and (b) methyl blue onto montmorillonite clay at different temperature. Initial dye concentration: 0.2 mM, Concentration of clay suspension: 100 mgL^{-1}, pH 5, total volume 200 mL. (The results are average of triplicate experiments and the error bar is shown for reference.)

The ΔG° value was calculated using Eq. (5). The Vant Hoff plot was generated by plotting ln (1,000 K_d) vs. $1/T$ for determination of the ΔH° and ΔS° values and presented in Fig. 10. The values of thermodynamic parameters obtained using these equations are given in Table 3. The negative ΔG° values indicate the spontaneity of the process. The numerical value of ΔG° are very close to the characteristic range of physisorption which is reported to be (0 to −20) kJ/mol [11,26,27] and are significantly lower than that of chemisorption which is reported to be (−80 to −400) kJ/mol [26]. Table 3 shows that as temperature increases, the ΔG° value becomes more negative indicating increase of adsorption capacity with temperature. The ΔH° values are also in the range of physisorption process which is reported to be 1–93 kJ/mol [28]. The positive value of ΔH° indicates endothermic nature of the adsorption process [26–28]. The increased randomness at the clay–water interface and good affinity of the dye molecules towards montmorillonite clay is proved by the positive ΔS° value [23]. The thermodynamic parameters of the present adsorption process is similar to the previous results obtained by this group and also many other literatures [9,10,23].

3.4. Activation energy

The adsorption process was further characterized by determining the activation energy, E_a, of the adsorption process using Arrhenius equation [29]. The activation energy of the adsorption of methyl green and methyl blue onto montmorillonite clay were found to be 23.212 and 9.486 kJ/mol as calculated from the slope of the Arrhenius plot. The low value of activation energy also suggests that the adsorption is governed by physisorption process (Fig. 11) [29].

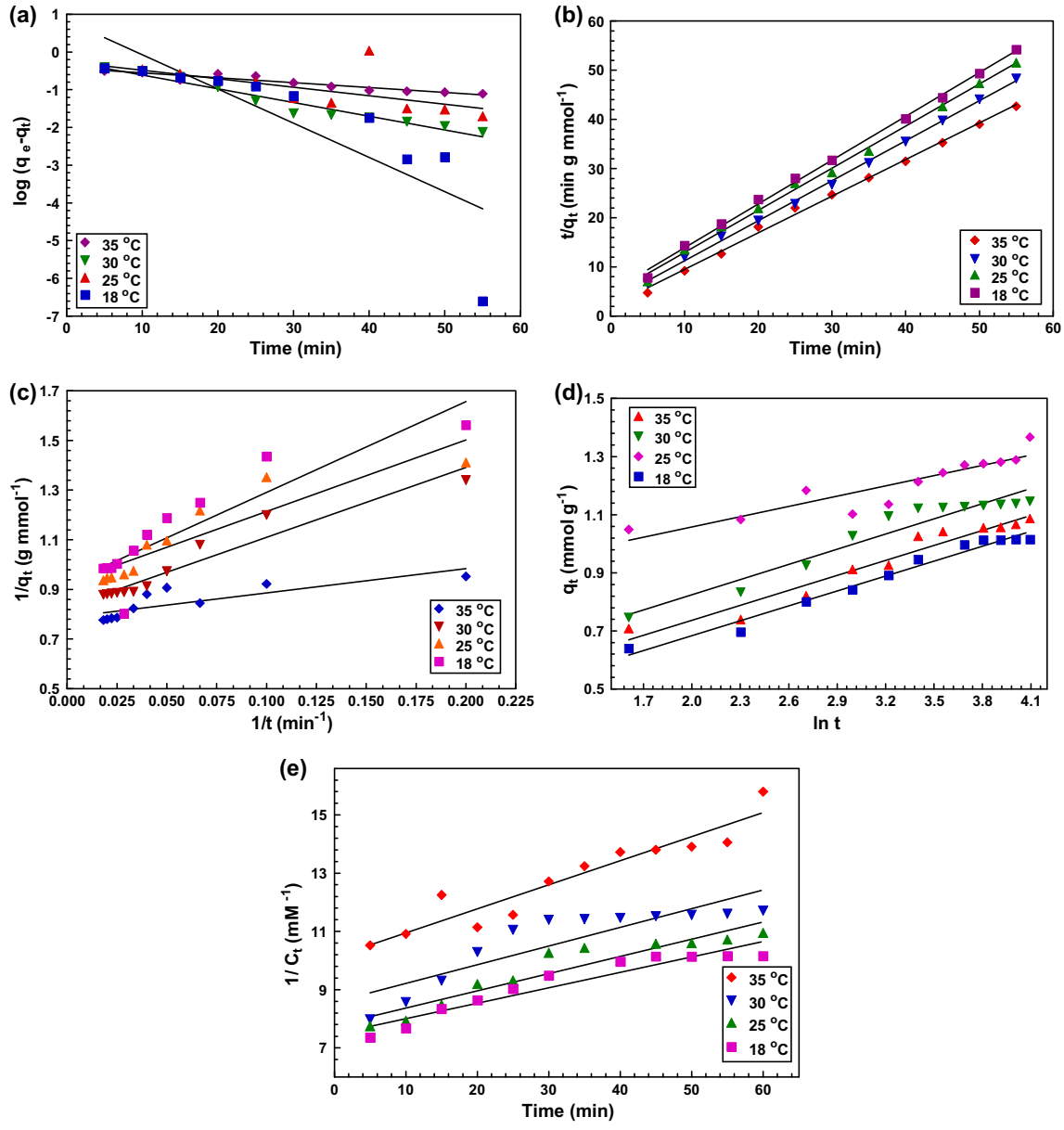

Fig. 7. Plots for kinetic models for adsorption of methyl green onto montmorillonite clay (a) pseudo-first-order (b) linear pseudo-second-order (c) pseudo-second-order (non-linear) (d) Elovich and (e) Bajpai model.

3.5. Adsorption isotherm

The adsorption isotherm experiments were carried out for adsorption of methyl green and methyl blue dye molecules at five different pHs namely 4, 5, 6, 7, 9, and at 25°C. The adsorption equilibrium data were analyzed using different isotherm models such as Langmuir, Freundlich, Sips, Toth, Temkin, Scatchard, and Dubinin and Radushkevich (D–R) models and are presented in Figs. 12(a)–(g) and 13(a)–(g), respectively [30–34]. The isotherm parameters obtained from these models are presented in Table 4. The used models are summarized in Table 5. The values of R^2 for the isotherm plots indicate that the Toth isotherm is the best fit model for both the dye molecules. The fitting of the adsorption isotherm data to Toth isotherm model suggests that the adsorption energy of most sites of the montmorillonite clay consists of less energy than mean adsorption energy [35].

It is observed from the Figs. 12 and 13 that the adsorption capacity of methyl green onto the clay

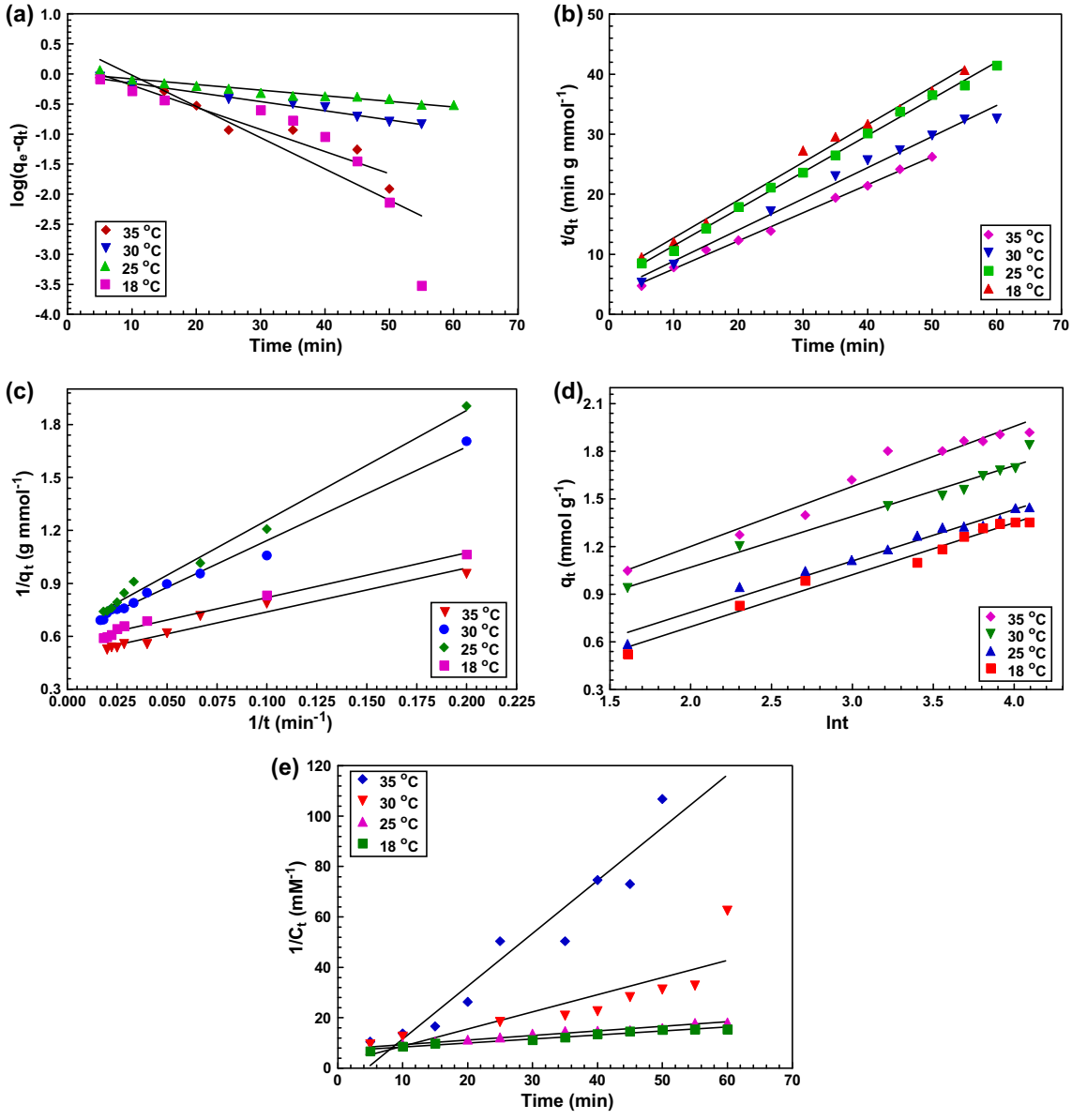

Fig. 8. Plots for kinetic models for adsorption of methyl blue onto montmorillonite clay (a) pseudo-first-order (b) linear pseudo-second-order (c) pseudo-second-order (non-linear) (d) Elovich and (e) Bajpai model.

increases and that of methyl blue onto the clay decreases with increase of initial pH of the suspension. At low pH, there is a high abundance of positively charged H^+ ions on the clay–water suspension which imparts a repulsive force towards the positively charged methyl green dye molecule. As the pH increases, amount of OH^- ions also increases. As a result, the amount of negative charge on the suspension also increases which facilitates the adsorption of the methyl green dye molecule onto the montmorillonite clay. On the other hand, the adsorption of anionic methyl blue dye molecule is more at lower pH due to the high abundance of positive charge in the suspension which decreases with increase in pH due to the repulsive force of negative charges at higher pH. The adsorption capacity of the methyl green dye molecule onto montmorillonite clay was found to be 3.976 mmol/g which is 49.120% more than that onto

Table 1
The kinetic model parameters for adsorption of methyl green and methyl blue onto the montmorillonite clay

Dye molecule									
		Methyl green				Methyl blue			
Models	Parameters	T (°C)							
		18	25	30	35	18	25	30	35
	$q_{e,exp}$ (mmol/g)	1.015	1.087	1.146	1.367	1.352	1.447	1.840	1.919
Pseudo-first-order	K_1 (min^{-1})	1.932	0.593	0.576	0.973	0.120	0.022	0.035	0.107
	$q_{e,cal}$ (mmol/g)	6.899	0.552	0.562	0.378	3.180	1.028	1.004	1.437
	R^2	0.696	0.448	0.951	0.909	0.738	0.938	0.981	0.568
Pseudo-second-order (linear)	K_2 (L/(mol min))	0.159	0.167	0.207	0.271	0.061	0.070	0.073	0.074
	$q_{e,cal}$ (mmol/g)	1.123	1.168	1.230	1.344	1.590	1.634	1.929	2.142
	R^2	0.998	0.996	0.998	0.997	0.993	0.997	0.988	0.997
Pseudo-second-order (non-linear)	$K_{2n,l}$ (mmol/(L min))	0.233	0.297	0.245	0.638	0.065	0.070	0.126	0.097
	$q_{e,cal}$ (mmol/g)	1.081	1.080	1.205	1.268	1.573	1.636	1.768	2.042
	R^2	0.800	0.827	0.930	0.675	0.991	0.988	0.988	0.951
Elovich	α (mg/g min)	1.054	1.689	2.682	124.932	0.371	0.498	1.217	1.223
	β (g/mg)	5.847	5.814	5.747	8.475	3.049	3.096	3.116	2.646
	R^2	0.975	0.948	0.930	0.835	0.982	0.977	0.973	0.958
Richi	K_i	0.253	0.321	0.296	0.810	0.102	0.115	0.223	0.197
	$q_{e,cal}$ (mmol/g)	1.081	1.080	1.205	1.268	1.573	1.636	1.768	2.042
	R^2	0.252	0.321	0.295	0.809	0.991	0.988	0.988	0.951
Bajpai	K_b	0.007	0.008	0.007	0.008	0.023	0.024	0.356	0.222
	$C_{0,cal}$ (mM)	0.134	0.129	0.117	0.099	0.147	0.134	0.523	0.106
	R^2	0.663	0.719	0.672	0.832	0.965	0.963	0.707	0.949

rGO (adsorption capacity: 2.023 mmol/g) and 38.229% less than that onto GO (adsorption capacity: 5.496 mmol/g). The adsorption capacity of the methyl blue dye molecule onto montmorillonite clay was found to be 5.105 mmol/g which is 20.078% more than that onto GO (adsorption capacity: 4.080 mmol/g) and 14.829% less than that onto rGO (adsorption capacity: 5.862 mmol/g).

3.6. Effect of presence of other ions on adsorption

The effect of presence of different ions such as Na^+, Ca^{2+}, Mg^{2+}, and SO_4^{2-} on adsorption isotherms of methyl green and methyl blue onto montmorillonite clay was studied at pH 5 and 30°C and the results are presented in Fig. 14. Fig. 14 shows that the adsorption capacity of methyl green dye molecule onto montmorillonite clay increases in presence of SO_4^{2-} ion and decreases in presence of the cations in the order: without salt > Na^+ > Ca^{2+} > Mg^{2+}. As discussed earlier, methyl green is a cationic dye molecule. Presence of the cations at the clay–water interfaces imparts a repulsive force to the cationic dye molecule and thereby decreasing the adsorption capacity of methyl green onto montmorillonite clay. The divalent cations (Ca^{2+}, Mg^{2+}) impart greater shielding effect than monovalent ions (Na^+) on the adsorption of methyl green onto the montmorillonite clay due to their high polarizing power [36]. The adsorption capacity of methyl green on the montmorillonite clay is higher in presence of SO_4^{2-} ions than without salt. Presence of SO_4^{2-} ions increases the negative charge on the solution which favors the adsorption of cationic dye molecule onto montmorillonite clay. On the other hand, the adsorption capacity of methyl blue dye molecule increases in presence of the ions in the order without salt < SO_4^{2-} < Na^+ < Ca^{2+} < Mg^{2+}. As methyl blue is an anionic dye, presence of the cations at clay–water

Table 2
Summary of adsorption kinetic models used in the present study

Sl. No.	Models
1.	Pseudo-first-order kinetics $\log (q_e - q_t) = \log q_e - (k_1 t/2.303)$ where k_1: Rate constant of the pseudo-first-order kinetic equation q_t: Adsorption capacity of dye molecules at time t q_e: Adsorption capacity of dye molecules at equilibrium
2.	Pseudo-second-order (linear) kinetics $t/q_t = 1/k_2 q_e^2 + 1/q_e t$ where, k_2: Rate constant of the pseudo-second-order kinetic equation
3.	Pseudo-second-order (non-linear) kinetics $q_t = k_{nl} q_e^2 t/(k_{nl} q_e t + 1)$ where, k_{nl}: Rate constant of the pseudo-second-order kinetic equation in non-linear form
4.	Elovich kinetics model $q_t = (1/\beta)\ln\alpha\beta + (1/\beta)\ln t$ where, α: Initial adsorption rate β: Elovich coefficient related to the extent of surface coverage and activation energy
5.	Richie kinetics model $q_t = q_e k_i t/(k_i t + 1)$ where, k_i: Rate constant of the Richie kinetic equation
6.	Bajpai model $1/C_t = k_I t/C_0 + 1/C_0$ where, k_I: Rate constant of the Bajpai kinetic equation C_0: Concentration of dye at time, $t = 0$ C_t: Concentration of dye at time, t

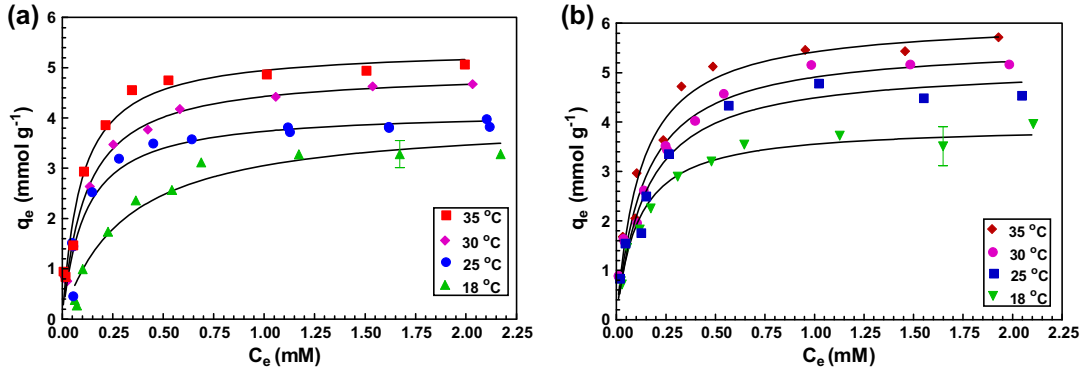

Fig. 9. Plot of equilibrium adsorption capacity vs equilibrium concentration for adsorption of (a) methyl green and (b) methyl blue onto montmorillonite clay at different temperatures (pH 5). (The results are average of triplicate experiments and the error bar is shown for reference.)

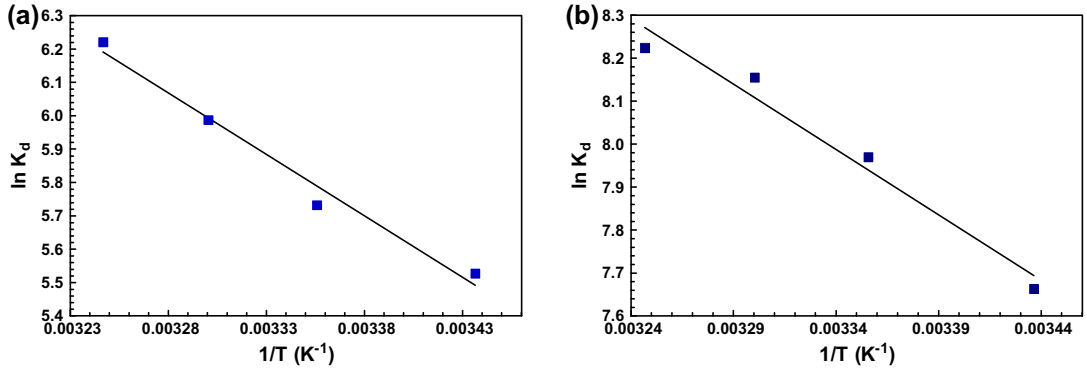

Fig. 10. Vant Hoff plot for adsorption of (a) methyl green and (b) methyl blue onto montmorillonite clay.

Table 3
Thermodynamic parameters for the adsorption of methyl green and methyl blue onto montmorillonite clay

	Dye molecules					
	Methyl green			Methyl blue		
T(°C)	ΔG° (kJ/mol)	ΔH° (kJ/mol)	ΔS° (kJ/mol K)	ΔG° (kJ/mol)	ΔH° (kJ/mol)	ΔS° (kJ/mol K)
18	−20.3683	30.628	18.15	−18.541	25.282	0.150
25	−21.3656			−19.7465		
30	−22.3665			−20.5441		
35	−23.3328			−21.0602		

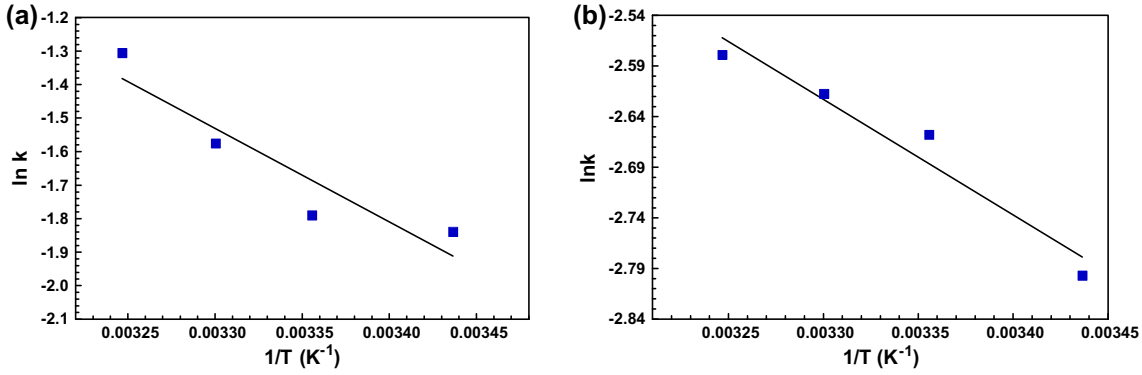

Fig. 11. Arrhenius plot for adsorption of (a) methyl green and (b) methyl blue onto montmorillonite clay.

interface facilitates the adsorption process. The adsorption capacity increases in presence of SO_4^{2-} ions due to the presence of Na^+ ions as the salt used was Na_2SO_4. The increase is not so much recordable due to the repulsive force of SO_4^{2-} ions. Presence of Cl^- ions in the other salts have negligible effect due to its lower polarizability than SO_4^{2-} ions (Cl^- = 3.76 Å^3, SO_4^{2-} = 6.33 Å^3) [35]. However, in case of adsorption of methyl blue onto GO and rGO nanosheets effect of presence of other ions is more prominent. The maximum adsorption capacity of methyl blue onto GO and rGO nanosheets in presence of Mg^{2+} ions was found to be 133.165 and 103.172% higher than that onto montmorillonite clay.

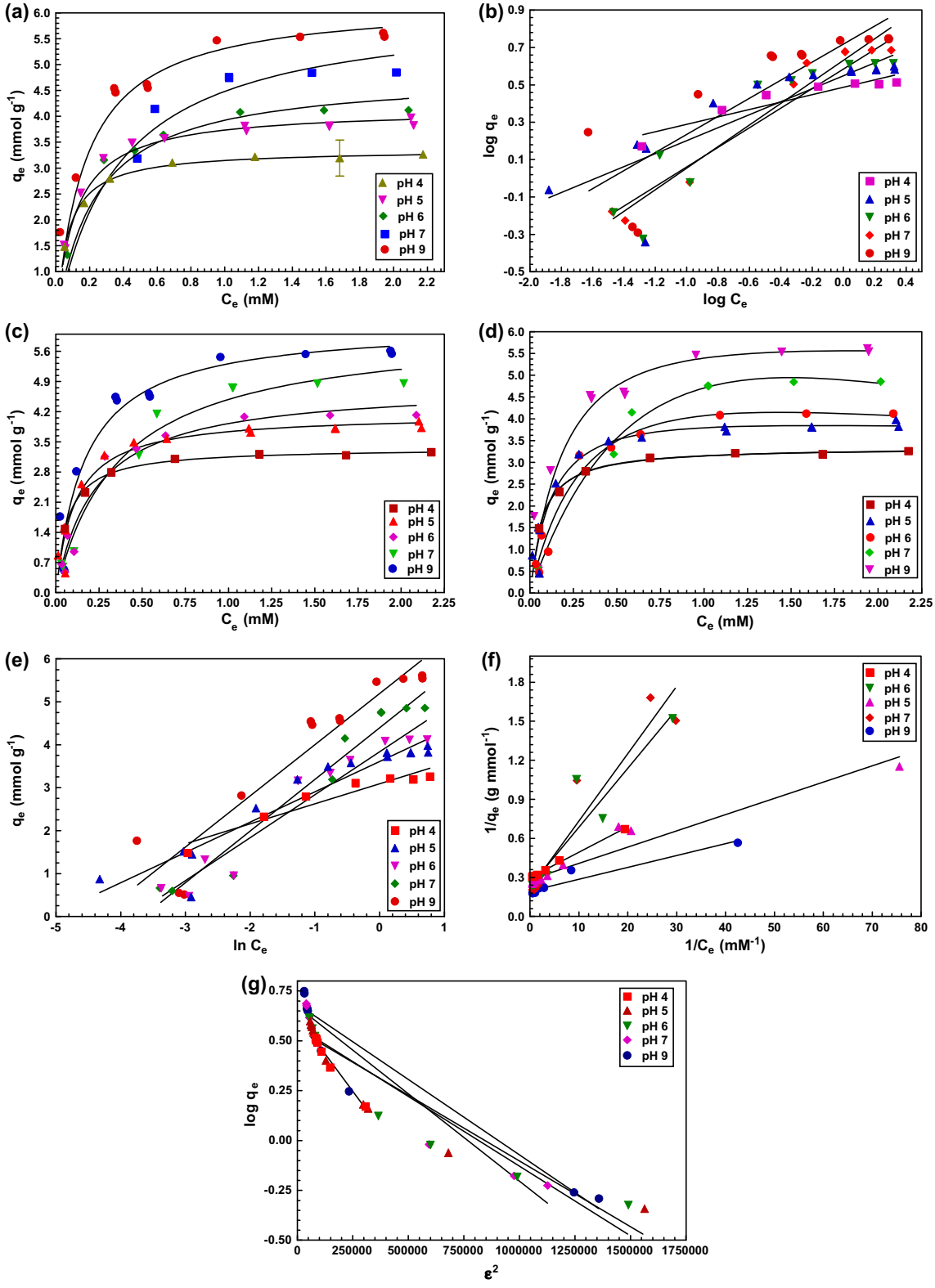

Fig. 12. Isotherm plots for adsorption of methyl green onto montmorillonite clay (a) Langmuir, (b) Freundlich, (c) Sips, (d) Toth, (e) Temkin, (f) Scatchard, and (g) D–R model. (The results are average of triplicate experiments and the error bar is shown for reference.)

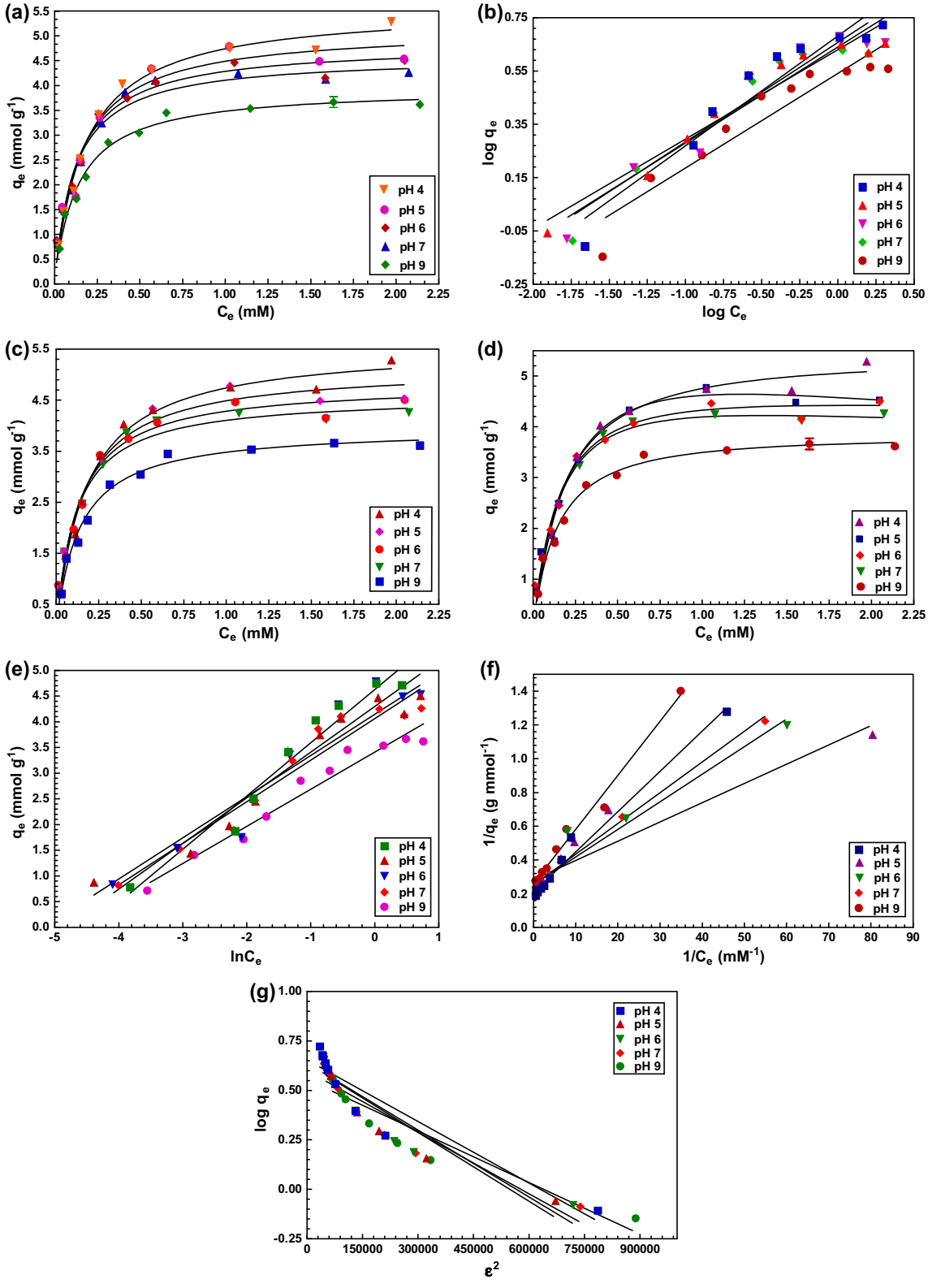

Fig. 13. Isotherm plots for adsorption of methyl blue onto montmorillonite clay (a) Langmuir, (b) Freundlich, (c) Sips, (d) Toth, (e) Temkin, (f) Scatchard, and (g) D–R model. (The results are average of triplicate results and error bar is shown for reference.)

Table 4
Parameters of the isotherm models for the adsorption of methyl green and methyl blue onto montmorillonite clay at different pH

Dye molecule											
Models	Parameters	Methyl green					Methyl blue				
		pH 4	pH 5	pH 6	pH 7	pH 9	pH 4	pH 5	pH 6	pH 7	pH 9
	Q_{0exp} (mmol/g)	3.372	4.148	4.821	6.140	6.226	5.168	4.912	4.521	4.394	3.765
Langmuir	Q_0 (mmol/g)	3.218	3.976	4.122	4.854	5.614	5.572	5.105	4.787	4.642	3.951
	K_L (L/mmol)	14.633	9.050	4.382	2.709	5.811	5.711	6.766	7.981	8.258	7.348
	R^2	0.996	0.941	0.958	0.978	0.932	0.987	0.954	0.972	0.972	0.989
Freundlich	$1/n$	0.198	0.347	0.524	0.577	0.484	0.412	0.336	0.361	0.373	0.355
	K_F (mmol/g)(mmol/L)$^{1/n}$	3.077	3.583	3.851	4.268	5.230	4.801	4.270	4.368	4.540	3.479
	R^2	0.873	0.743	0.857	0.961	0.708	0.917	0.929	0.921	0.919	0.893
Sips	Q_0 (mmol/g)	3.372	4.148	4.821	6.140	6.226	5.572	5.105	4.787	4.642	3.951
	K_s (L/mmol)	1.050	1.062	1.227	0.822	0.873	1.113	1.052	1.059	1.063	1.073
	S	0.072	0.117	0.280	0.304	0.150	0.195	0.156	0.133	0.129	0.146
	R^2	0.996	0.941	0.958	0.978	0.932	0.987	0.954	0.972	0.972	0.989
Toth	Q_0 (mmol/g)	3.432	5.849	12.870	73.161	9.809	6.149	11.690	6.502	7.500	4.417
	K_T (mmol/g)	14.25	6.182	1.843	0.415	3.630	5.143	3.041	5.616	4.802	6.475
	T	1.004	1.097	1.379	2.607	1.144	1.028	1.260	1.088	1.144	1.031
	R^2	0.996	0.944	0.969	0.990	0.937	0.987	0.962	0.974	0.977	0.989
Temkin	A	769.054	165.985	46.201	38.572	77.791	86.569	175.856	126.205	152.225	112.513
	B (g/mmol)	0.465	0.706	1.000	1.203	1.192	1.037	0.802	0.888	0.808	0.722
	R^2	0.920	0.898	0.935	0.957	0.894	0.964	0.939	0.929	0.936	0.959
Scatchard	Q_0 (mmol/g)	3.348	3.516	4.275	4.615	5.040	4.760	3.539	3.922	3.960	3.840
	K_s (L/mmol)	15.287	22.807	5.168	4.193	21.367	8.813	24.746	15.605	13.858	8.135
	R^2	0.997	0.931	0.892	0.925	0.933	0.983	0.896	0.943	0.976	0.986
D–R	Q_0 (mmol/g)	4.218	3.612	3.722	4.704	4.830	4.523	4.323	4.357	3.975	3.595
	K_{D-R} (mol/kJ)^2	1.513×10^{-7}	6.605×10^{-7}	6.992×10^{-7}	8.754×10^{-7}	7.554×10^{-7}	1.039×10^{-6}	1.159×10^{-6}	1.129×10^{-6}	1.036×10^{-6}	0.869×10^{-6}
	E (kJ/mol)[a]	1.817	0.870	0.845	0.755	0.813	0.693	0.656	0.665	0.694	0.758
	R^2	0.979	0.868	0.906	0.957	0.933	0.884	0.900	0.877	0.880	0.936

[a]$E = 1/(2K_{D-R})^{1/2}$.

Table 5
Summary of adsorption isotherm models used in the present study

Sl. No	Models
1.	*Langmuir* $C_e/q_e = 1/Q_0K_L + (1/Q_0)C_e$ where, K_L: Langmuir constant related to the energy of adsorption Q_0: Maximum adsorption density
2.	*Freundlich* $q_e = K_F C_e^{1/n}$ where, K_F: Freundlich constant related to adsorption capacity n: Freundlich constant related to adsorption intensity
3.	*Sips* $q_e = Q_0(K_sC_e)^{1/s}/[1 + (K_sC_e)^{1/s}]$ where, K_s: Sips equilibrium constant related to adsorption affinity S: Heterogeneity factor
4.	*Toth* $q_e = Q_0K_TC_e/ [(1 + K_TC_e)^t]^{1/t}$ where, K_s: Toth constant t: Heterogeneity factor
5.	*Temkin* $q_e = B \ln A + B \ln C_e$ where, B = RT/b; B: Temkin constant A: Temkin isotherm constant
6.	*Scatchard* $C_e/q_e = K_s (Q_0 - q_e)$ where, K_s: Adsorption isotherm parameter
7.	*Dubinin and Radushkevich (D–R)* $q_e = q_{max}\exp(-K_{DR}\varepsilon^2)$ where, $K_{D–R}$: Adsorption constant $\varepsilon = RT \log(1 + 1/C_e)$

3.7. Mechanism of adsorption

To study the mechanism of adsorption of the dye molecules onto montmorillonite clay FTIR spectroscopic and XRD analysis of the montmorillonite clay before and after adsorption of dye molecules was carried out.

3.7.1. FTIR analysis

The bands in the FTIR spectrum of montmorillonite clay are assigned in characterization section. Assignment of the bands of methyl green and methyl blue dye molecules are described in our previous publications [9,10]. The intensity of the band at 1,057 cm^{-1} of FTIR spectrum of montmorillonite clay due to Si–O–Si stretching decreases after adsorption of methyl green dye molecule (Fig. 15(a)). This indicates involvement of electrostatic interaction between the $(=NH)^+$ groups with negatively polar oxygen moiety of SiO_2 groups of montmorillonite clay. On the other hand, the intensity of band at 1,346 cm^{-1} corresponds to SO_3^- groups of methyl blue dye molecule decreases and another band at 1,163 cm^{-1} due to same group disappears after getting adsorbed onto montmorillonite clay (Fig. 15(b)). This indicates interaction between the negatively charged SO_3^- groups with Al^{3+} groups of montmorillonite clay. Similar interaction is also reported by Errais et al. for adsorption of anionic RR120 dye molecules onto clay minerals [3].

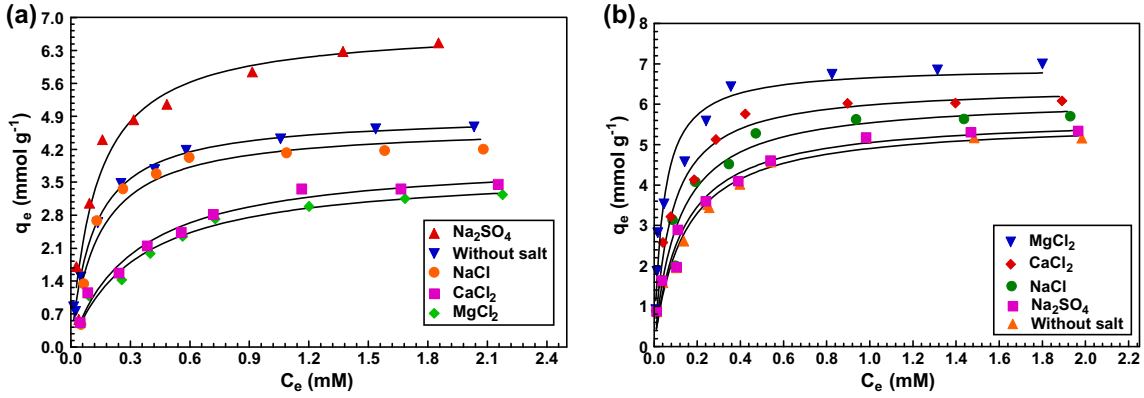

Fig. 14. Plot of equilibrium adsorption capacity vs equilibrium concentration for adsorption of (a) methyl green and (b) methyl blue onto montmorillonite clay in presence of different ions (30°C, pH 5).

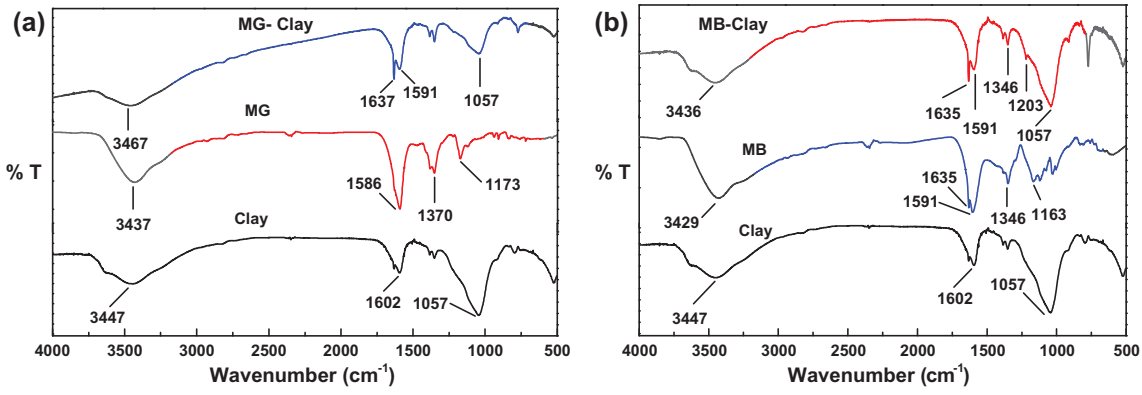

Fig. 15. FTIR spectra of (a) montmorillonite clay (clay), methyl green (MG), and methyl green adsorbed clay (MG–clay) and (b) montmorillonite clay (clay), methyl blue (MB), and methyl blue adsorbed clay (MB–clay).

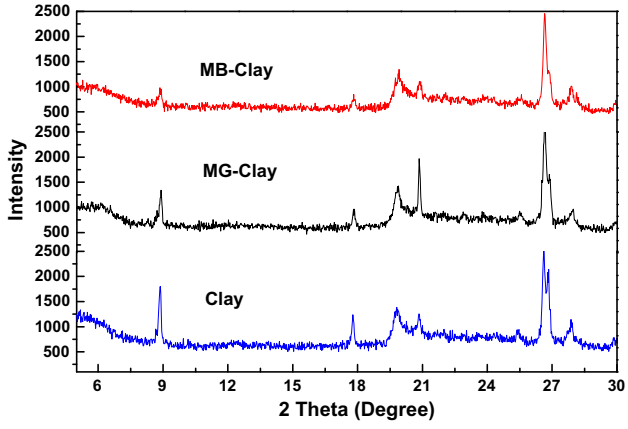

Fig. 16. XRD pattern of montmorillonite clay before dye adsorption (Clay), after adsorption of methyl green (MG–Clay) and after adsorption of methyl blue (MB–Clay).

3.7.2. XRD analysis

The raw montmorillonite clay shows a peak for (0 0 1) plane at $2\theta = 8.880$ with d spacing value of 9.9500 (Fig. 16) which increases up to 10.1322 and 9.9724 after adsorption of methyl green and methyl blue, respectively. Such increase in the d—spacing value indicates the insertion of these dye molecules into the interlayer spacing of the clay [7].

3.7.3. Comparative study

The adsorption efficiency of the adsorption of methyl green and methyl blue dye molecules onto montmorillonite clay has been compared with other adsorbent materials available in literature. The results are presented in Table 6. It was observed from Table 6 that montmorillonite clay, under our experimental conditions shows good efficiency which is even better than numbers of other adsorbent materials for both the dye molecules.

Table 6
Comparison of adsorption efficiency of methyl green and methyl blue dye molecules onto different adsorption materials

Dye molecules	Adsorbents	Adsorption efficiency (%)	References
Methyl green	$NiFe_2O_4$–carbon nanotube composites	56	[37]
Methyl green	Carbon nanotube	60	[37]
Methyl green	Montmorillonite	67	[8]
Methyl green	Cross-linked amphoteric starch	84	[38]
Methyl green	Graphene oxide	93	[10]
Methyl green	Montmorillonite	68	This study
Methyl blue	Magnetic charcoal	64	[39]
Methyl blue	rGO	85	[7]
Methyl blue	GO	58	[9]
Methyl blue	Montmorillonite	96	This study

4. Conclusions

This study shows that methyl green and methyl blue dye molecules can be successfully removed from water system by adsorption onto montmorillonite clay. Temperature and pH of the solution have the major impact on the adsorption capacity of the dye molecules onto the clay. Negative value of Gibbs free energy indicates the spontaneity of the process. The values of ΔH°, ΔS°, E, and increase of adsorption capacity with temperature prove that the adsorption is governed by physisorption. FTIR analysis indicates involvement of electrostatic interaction between the functional groups of the dye molecules with montmorillonite clay. XRD analysis shows the insertion of the dye molecules into the interlayer spacing of the clay. The adsorption capacity of methyl green onto montmorillonite clay increases in presence of anions and decreases in presence of cations. The adsorption capacity of methyl blue onto montmorillonite clay increases in presence of the ions. The adsorption efficiency of methyl blue dye molecule onto montmorillonite clay is found to be higher than that of methyl green onto montmorillonite clay. A removal of methyl green and methyl blue dye molecules up to 68.35 and 95.95%, respectively was achieved at pH 5 and 35°C by this method. This study will be helpful for optimizing the adsorption parameters for effective removal of dye molecules from aqueous system using clay based adsorbent materials.

Acknowledgments

The authors are thankful to the Director, CSIR-NEIST, Jorhat for his interest to carry out the work. PS acknowledges to CSIR, New Delhi for SRF grant.

References

[1] M.M. Ayad, A.E.N. El-Nasr, Adsorption of cationic dye methylene blue from water using polyaniline nanotubes base, J. Phys. Chem. C 114 (2010) 14377–14383.
[2] Y.C. Wong, Y.S. Szeto, W.H. Cheung, G. Mckey, Equilibrium studies for acid dye adsorption onto chitosan, Langmuir 19 (2003) 7888–7894.
[3] E. Errais, J. Duplay, M. Elhabiri, M. Khodja, R. Ocampo, R.B. Guyot, F. Darragi, Anionic RR120 dye adsorption onto raw clay: Surface properties and adsorption mechanism, Colloid Surf., 403 (2012) 69–78.
[4] D. Chen, J. Chen, X. Luan, H. Ji, Z. Xia, Characterization of anion–cationic surfactants modified montmorillonite and its application for the removal of methyl orange, Chem. Eng. J. 171 (2011) 1150–1158.
[5] S. Çoruh, F. Geyikçi, Adsorption of copper (II) ions on montmorillonite and sepiolite clays: Equilibrium and kinetic studies, Desalin. Water Treat. 45 (2012) 351–360.
[6] S. Çoruh, O.N. Ergun, Ni^{2+} removal from aqueous solutions using conditioned clinoptilolites: Kinetic and isotherm studies, Environ. Prog. Sustainable Energy 28 (2009) 162–172.
[7] M. Roulia, A.A. Vassiliadis, Interactions between C.I. Basic Blue 41 and aluminosilicate sorbents, J. Colloid Interface Sci. 291 (2005) 37–44.
[8] G. Rytwo, S. Nir, M. Crespin, L. Margulies, Adsorption and Interactions of Methyl green with Montmorillonite and Sepiolite, J. Colloid Interf. Sci. 222 (2000) 12–19.
[9] P. Sharma, N. Hussain, D.J. Borah, M.R. Das, Kinetics and adsorption behavior of the methyl blue at the graphene oxide/reduced graphene oxide nanosheet–water interface: A comparative study, J. Chem. Eng. Data 58 (2013) 3477–3488.
[10] P. Sharma, M.R. Das, Removal of a cationic dye from aqueous solution using graphene oxide nanosheets: Investigation of adsorption parameters, J. Chem. Eng. Data 58 (2013) 151–158.
[11] X.Y. Pang, F. Gong, Study on the adsorption kinetics of acid red 3B on expanded graphite, E-J. Chem. 5 (2008) 802–809.

[12] P.S. Bradder, S.K. Ling, S. Wang, S. Liu, Dye adsorption on layered graphite oxide, J. Chem. Eng. Data 56 (2011) 138–141.
[13] G.K. Ramesha, A.V. Kumara, H.B. Muralidhara, S. Sampath, Graphene and graphene oxide as effective adsorbents toward anionic and cationic dyes, J. Colloid Interface Sci. 361 (2011) 270–277.
[14] T. Liu, Y.D.Q. Li, J. Sun, Y. Jiao, G. Yang, Z. Wang, Y. Xia, W. Zhang, K. Wang, H. Zhu, D. Wu, Adsorption of methylene blue from aqueous solution by graphene, Colloids Surf. B 90 (2012) 197–203.
[15] C.J. Ogugbue, T. Sawidis, Bioremediation and detoxification of synthetic wastewater containing triarylmethane dyes by aeromonas hydrophila isolated from industrial effluent, Biotech. Res. Int. (2011) 967925–967935.
[16] A. Ghebaur, S.A. Gârea, H. Iovu, The influence of inorganic host type in the drug—Layered silicate biosystems, U.P.B. Sci. Bull. Series B 73 (2011) 169−176.
[17] S. Lagergren, About the theory of so-called adsorption of soluble substances, K. Sven. Vetenskapsakad. Handl. 24 (1898) 1–39.
[18] Y.S. Ho, G. McKay, Sorption of dye from aqueous solution by peat, Chem. Eng. J. 70 (1998) 115–124.
[19] J.M. Borah, J. Sarma, S. Mahiuddin, Adsorption comparison at the α-alumina/water interface: 3,4-Dihydroxybenzoic acid vs. catechol, Colloids Surf. A 387 (2011) 50–56.
[20] L. Guo, G. Li, J. Liu, S. Ma, J. Zhang, Kinetic and equilibrium studies on adsorptive removal of toluidine blue by water-insoluble starch sulfate, J. Chem. Eng. Data 56 (2011) 1875–1881.
[21] J.M. Borah, M.R. Das, S. Mahiuddin, Influence of anions on the adsorption kinetics of salicylate onto α-alumina in aqueous medium, J. Colloid. Interface Sci. 316 (2007) 260–267.
[22] M.R. Das, S. Mahiuddin, The influence of functionality on the adsorption of p-hydroxy benzoate and phthalate at the hematite–electrolyte interface, J. Colloid. Interface Sci. 306 (2007) 205–215.
[23] L. Ai, M. Li, L. Li, Adsorption of methylene blue from aqueous solution with activated carbon/cobalt ferrite/alginate composite beads: Kinetics, isotherms, and thermodynamics, J. Chem. Eng. Data 56 (2011) 3475–3483.
[24] K.M. Slobodan, A consideration of the correct calculation of thermodynamic parameters of adsorption, J. Serb. Chem. Soc. 72 (2007) 1363–1367.
[25] Y. Liu, Is the free energy change of adsorption correctly calculated, J. Chem. Eng. Data 54 (2009) 1981–1985.
[26] C.H. Weng, Y.T. Lin, T.W. Tzeng, Removal of methylene blue from aqueous solution by adsorption onto pineapple leaf powder, J. Hazard. Mater. 170 (2009) 417–424.
[27] A.N. Fernandes, C.A.P. Almeida, N.A. Debacher, M.D.S. Sierra, Isotherm and thermodynamic data of adsorption of methylene blue from aqueous solution onto peat, J. Mol. Struct. 982 (2010) 62–65.
[28] M. Hema, S. Arivoli, Rhodamine B adsorption by activated carbon: Kinetic and equilibrium studies, Indian J. Chem. Technol. 16 (2009) 38–45.
[29] S. He, Y. Zhou, Z. Gu, S. Xie, X. Du, Adsorption of two cationic dyes from aqueous solution onto natural attapulgite, 3rd Int. Conf. Bioinformatics Biomed. Eng. (ICBBE) (2009 June) 11–13.
[30] I. Langmuir, The adsorption of gases on plane surfaces of glass, mica and platinum, J. Am. Chem. Soc. 40 (1918) 1361–1403.
[31] H.M.F. Freundlich, Over the adsorption in solution, Z. Phys. Chem. 57 (1906) 385–470.
[32] X.S. Wang, Y. Qin, Equilibrium sorption isotherms for of Cu^{2+} on rice bran, Process Biochem. 40 (2005) 677–680.
[33] T.S. Anirudhan, P.S. Suchithra, Equilibrium, kinetic and thermodynamic modeling for adsorption of heavy metals onto chemically modified hydrotelcite, Indian J. Chem. Technol. 17 (2010) 247–259.
[34] M.R. Das, J.M. Borah, W. Kunz, B.W. Ninham, S. Mahiuddin, Ion specificity of the zeta potential of α-alumina, and of the adsorption of p-hydroxybenzoate at the α-alumina–water interface, J. Colloid Interface. Sci. 344 (2010) 482–491.
[35] Y.S. Ho, J.F. Porter, G. McKay, Equilibrium isotherm studies for the sorption of divalent metal ions onto peat: Copper, nickel and lead single component systems, Water Air Soil Pollut. 141 (2002) 1–33.
[36] N.C. Pyper, C.G. Pike, P.P. Edwards, The polarizabilities of species present in ionic solutions, Mol. Phys. 76 (1992) 353–372.
[37] M. Bahgat, A.A. Farghali, W. El Rouby, M. Khedr, M.Y.M. Ahmed, Adsorption of methyl green dye onto multi-walled carbon nanotubes decorated with Ni nanoferrite, Appl. Nanosci. 3 (2013) 251–261.
[38] S. Xu, J.l. Wang, R. Wu, J. Wang, H. Li, Adsorption behaviors of acid and basic dyes on crosslinked amphoteric starch, Chem. Eng. J., 117 (2006) 161–167.
[39] I. Šafařík, K. Nymburská, M. Šafaříková, Adsorption of water-soluble organic dyes on magnetic charcoal, J. Chem. Tech. Biotechnol. 69 (1997) 1–4.